Ratchet Effects Induced by Terahertz Radiation in Heterostructures with a Lateral Periodic Potential

P. Olbrich,[1] E. L. Ivchenko,[2] R. Ravash,[1] T. Feil,[1] S. D. Danilov,[1] J. Allerdings,[1] D. Weiss,[1] D. Schuh,[1] W. Wegscheider,[1] and S. D. Ganichev[1]

[1]*Terahertz Center, University of Regensburg, 93040 Regensburg, Germany*
[2]*A. F. Ioffe Physico-Technical Institute, Russian Academy of Sciences, 194021 St. Petersburg, Russia*
(Received 11 March 2009; published 28 August 2009)

We report on the observation of the Seebeck ratchet effect. The effect is measured in semiconductor heterostructures with a one-dimensional lateral potential excited by terahertz radiation. The photocurrent generation is based on the combined action of a spatially periodic in-plane potential and a spatially modulated light, which gives rise to a modulation of the local temperature. In addition to the polarization-independent current due to the Seebeck ratchet effect, we observe a photon helicity dependent response and propose a microscopic mechanism to interpret the experimental findings.

DOI: 10.1103/PhysRevLett.103.090603 PACS numbers: 05.40.−a, 05.60.Gg, 73.63.Hs, 78.67.De

Terahertz (THz) radiation incident on a two-dimensional electron system (2DES) generates a current whose direction depends on the symmetry of the system, the geometry, and the light's polarization state [1,2]. Nonequilibrium spatially periodic noncentrosymmetric systems are able to transport particles in the absence of an average macroscopic force. The directed transport in such systems, known as the ratchet effect, has a long history and is relevant to different fields of physics [3–11]. If this effect is induced by electromagnetic radiation it is usually referred to as a photogalvanic effect [12–14]. A novel situation emerges if a lateral superlattice (SL) is superimposed upon the 2DES: THz radiation, shining through a periodic grating, drives an additional current through the modulated 2DES. This directed current constitutes a ratchet effect which is closely related to the one investigated theoretically by Büttiker and Blanter [15]. These authors have shown that irradiation of a lateral SL by light through a mask with slits of the same period but with a shifted phase with respect to the SL results in a directed current due to local electron gas heating. In the experiment described below, the mask is replaced by a one-dimensional array of grooves etched into the top cap of a semiconductor heterostructure. The effect of the periodic grooves is twofold: (i) they generate a weak one-dimensional periodic potential superimposed upon the 2DES and (ii) they modulate, due to near-field diffraction [1], the intensity of the incident light field, which is hence spatially periodic in the plane of the 2DES. The modulated light field in turn causes a periodic modulation of the effective electron temperature. As the ratchet discussed below is based on a spatial modulation of the temperature it is called a Seebeck ratchet [5]. The phase shift of the mask relative to the periodic potential of the geometry of Blanter and Büttiker geometry is replaced by asymmetric grooves which have the same effect as a shifted phase and cause a directed current flow. Both geometries are compared in Figs. 1(a) and 1(b): The effect of the phase shifted mask in Fig. 1(a) is the same as the asymmetric profile of the grating in Fig. 1(b) as both cause a phase shift of the spatially periodic near-field intensity with respect to the periodic potential acting on 2DES. In addition, to this photothermal ratchet effect, which is manifested by a remarkable photocurrent for unpolarized radiation, we have observed in our experiments two additional photocurrent contributions being sensitive to the photon helicity and to the plane of linear polarization. Our theoretical analysis, expanding the one of Refs. [15] to the case of polarized radiation, enables us to propose new mechanisms of the observed effects.

We study photocurrents in (001)-GaAs/$Al_{0.3}Ga_{0.7}As$ MBE grown n-type quantum well (QW) structures with superimposed lateral grating. We used a single modulation-doped QW of 30 nm width, exhibiting at temperature $T = 4.2$ K (300 K) a mobility $\mu \approx 5 \times 10^6$ cm^2/V s ($\approx 6 \times 10^3$ cm^2/V s) at a carrier density $N \approx 2 \times 10^{11}$ cm^{-2} ($\approx 1.2 \times 10^{11}$ cm^{-2}). The values of electron mean free path, l_e, are ≈ 35 μm and 0.1 μm at $T = 10$ K and 300 K, respectively. One-dimensional grooves of 0.5 μm width with a period of 2.5 μm are obtained by electron beam lithography and transferred into the cap layer by subsequent reactive ion etching using $SiCl_4$. A corresponding electron micrograph is shown in Fig. 1(c). Care was taken not to etch through the QW. To get a large patterned area 64 squares, each 150×150 μm^2 in size, were

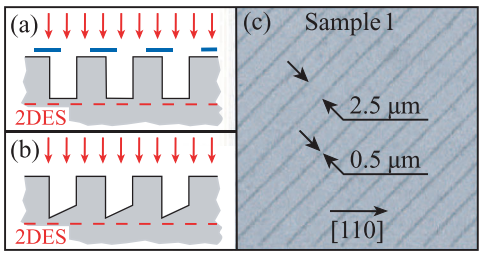

FIG. 1 (color). Sample design. (a) Blanter and Büttiker's geometry. (b) Our experimental geometry. (c) Electron micrograph.

stitched together. The gratings are oriented either along $\langle 010 \rangle$ (sample 1) or close to $\langle 110 \rangle$ (samples 2, 3) crystallographic directions. Below we will use the notation a for SL period and x, y for the in-plane axes oriented, respectively, perpendicular and parallel to the direction of the grating. Then the SL potential is a periodic function of x, namely, $V(x + a) = V(x)$. While the cross section of the grooves etched into the GaAs cap of samples 2 and 3 is essentially symmetric, the groove profile of sample 1 is asymmetric, Fig. 1(b). This asymmetry is due to the etching anisotropy along [110] and $[1\bar{1}0]$ directions [16]. We also prepared an unpatterned reference sample 4. The photocurrents were generated at $T = 300$ K and 10 K applying free carrier absorption of THz radiation. For optical excitation we used NH_3 laser [1] operating at a wavelength $\lambda = 280$ μm, with power $P \simeq 2$ kW and pulse duration $\approx$100 ns. The photocurrent was measured by the voltage drop across 50 Ω resistor using a pair of contacts centered on opposite sample edges (Fig. 2). The peak voltage was recorded with a storage oscilloscope. The radiation helicity was varied by using a $\lambda/4$ plate as $P_{\mathrm{circ}} = \sin 2\varphi$, where φ is the angle between the initial polarization plane and plate c axis.

First we discuss how the ratchet effect manifests itself in experiment. Figure 2 shows the photocurrent of sample 1 as a function of angle φ, assigning the helicity, for different angles of incidence θ_0 (Fig. 3). The photocurrent is maximal at normal incidence, which is in contrast to the unpatterned reference sample 4, where under normal incidence the signal vanishes (see inset of Fig. 2). Moreover, while under oblique incidence, the current in the reference sample follows a simple dependence $J = A_{\mathrm{ref}} \sin\theta_0 \sin 2\varphi$, the photocurrent behavior in the SL sample is more complex and can be fitted by

$$J = A \sin 2\varphi + B \sin 4\varphi + C \cos 4\varphi + D, \qquad (1)$$

where A, B, C, and D are fitting parameters. Such behavior, phenomenologically well described by symmetry arguments (see below) was found in all SL samples. In case of the reference sample 4 we observed that B, C, $D \approx 0$; furthermore, parameter A vanishes at $\theta_0 = 0$. In sample 1 with the grooves oriented along $\langle 010 \rangle$ the magnitude of the photocurrent detected at $\theta_0 = 0$ is comparable and even larger than the one obtained in the reference sample at large θ_0. The observed helicity dependence holds for the temperature range from 300 to 10 K. With decreasing temperature the photosignal increases, a corresponding trace taken at 10 K is included in Fig. 2. As the microscopic theory presented below is only applicable at elevated temperatures we focus in the following on room temperature data. In samples 2 and 3 with the grooves oriented along $\langle 110 \rangle$, however, the photocurrent at $\theta_0 = 0$ is about an order of magnitude smaller than that detected in sample 1. We ascribe this to the grooves profile being strongly asymmetric in sample 1 while nearly symmetric in samples 2 and 3.

Now we analyze our results from the viewpoint of phenomenological theory. Our unpatterned QWs have the point-group symmetry C_{2v} excluding in-plane photocur-

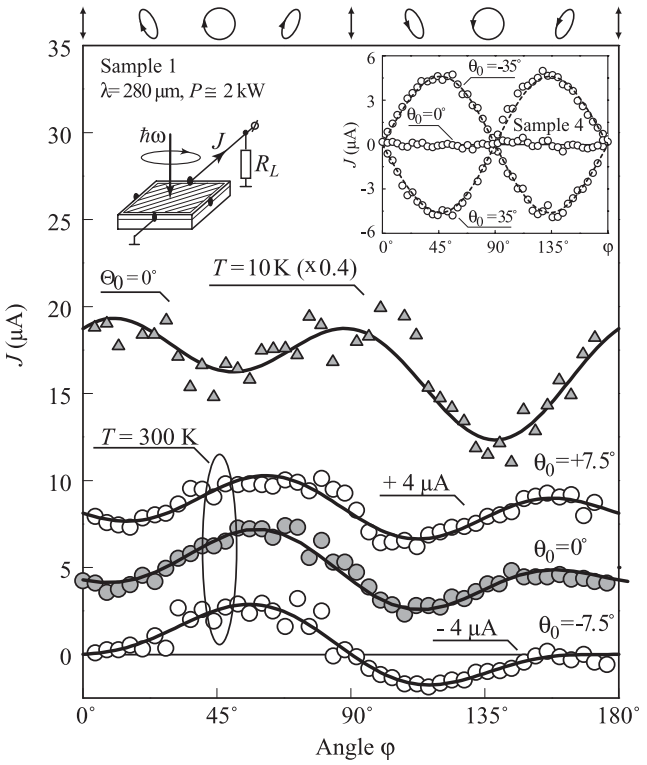

FIG. 2. Photocurrent as a function of the angle φ measured in sample 1. Full lines are fits to Eq. (1). Insets show the experimental geometry (left) and $J(\varphi)$ in the reference sample 4 (right). Doted lines are fits to $J = A_{\mathrm{ref}} \sin\theta_0 \sin 2\varphi$. The ellipses on top illustrate the polarization for various angles φ.

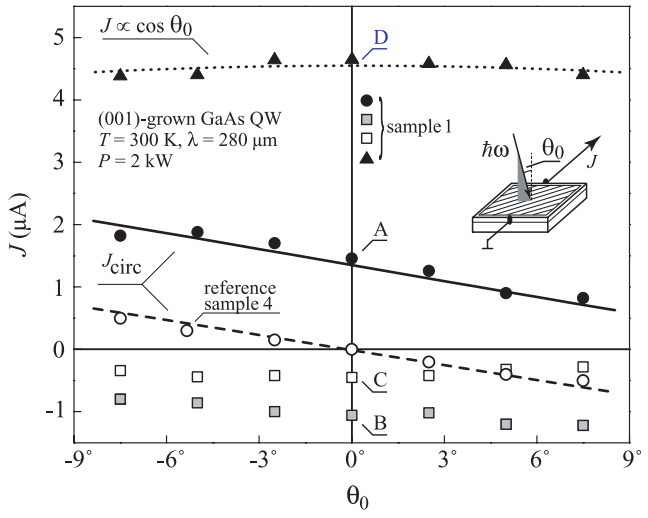

FIG. 3 (color online). Angle of incidence dependence of the photocurrent. ● and ○: J_{circ} measured in sample 1 and reference sample 4, respectively. ■, □, and ▲ are current contributions proportional to B, C, and D. Dotted line is the fit after $J = D\cos\theta_0$. Solid and dashed lines are fits to $J \propto (A_{\mathrm{ref}} \sin\theta_0 + A\cos\theta_0)$.

rents under normal incidence [1,17]. Indeed no current is observed in reference sample 4 at $\theta_0 = 0$ (see inset in Fig. 2). An asymmetric SL potential has the point-group symmetry C_s and overrides the C_{2v} symmetry of the underlying unpatterned QW. In such structures the normal-incidence excitation can induce photocurrents both along and normal to the grooves given by

$$\begin{aligned} j_x &= I[\chi_1 + \chi_2(|e_x|^2 - |e_y|^2)], \\ j_y &= I\chi_3(e_x e_y^* + e_y e_x^*) + I\gamma P_{\mathrm{circ}}, \end{aligned} \tag{2}$$

where e_x, e_y are the components of the light's polarization unit vector $\boldsymbol{e}$, I is the light intensity, χ_{1-3} and γ are phenomenological parameters. For the geometry used in experiment, in which the current is measured under an angle of 45° with respect to the axes x and y (see Fig. 2), the normal-incidence photocurrent is an equal superposition of the currents j_x and j_y. If the initial laser light is polarized along the line connecting the contacts then Eqs. (2) reduce to Eq. (1) with the coefficients $A = \gamma/\sqrt{2}$, $B = -\chi_2/2\sqrt{2}$, $C = \chi_3/2\sqrt{2}$, $D = C + \chi_1/\sqrt{2}$. From Eq. (2) it also follows that the linearly polarized radiation should yield a dc current which can be described, in terms of the coefficients entering Eq. (1), as $J = 2B\sin 2\alpha + 2C\cos 2\alpha + D - C$, where α is the azimuthal angle assigning the plane of polarization. Note that, the difference $D - C$ actually constitutes the polarization-independent ratchet effect proposed in [15]. We have checked experimentally (not shown) that, indeed, a photocurrent induced under linearly polarized excitation is well fitted by this equation.

Equations (2) yield the dependence of the photocurrent on the angle of incidence. In Fig. 3 we plot this dependence for all photocurrent contributions. The coefficients A, B, C, D are extracted from fits to the data of Fig. 2, using Eq. (1). Eye catching is the large value of D, which as well as B and C, is only weakly dependent on θ_0. Actually, the D portion of the current is the dominating one, has its maximum at normal incidence and can be well fitted by $J \propto \cos\theta_0$. The contributions given by the coefficients B and C are substantially smaller than D.

Next we compare the helicity dependent contribution of both the patterned sample 1 and the reference sample 4 under illumination with circularly polarized light. To extract the photon helicity dependent current from the total current we used the fact that this current changes its sign upon switching the helicity while all the other terms in Eq. (1) remain unchanged. Taking the difference of right- and left-handed photocurrents we obtain $J_{\mathrm{circ}} = [J(\varphi = 45°) - J(\varphi = 135°)]/2$. Figure 3 illustrates that J_{circ} in sample 1 consists of two contributions $(A_{\mathrm{ref}}\sin\theta_0 + A\cos\theta_0)$. Here the first term is the same as in the reference sample while the second term is a new contribution due to the lateral pattern.

Now we address the microscopic origin of the observed photocurrents at normal incidence and provide microscopic expressions for the relevant parameters χ_1 and γ. Here, we confine ourselves to the case of unpolarized (proportional to χ_1) and circularly polarized light (proportional to γ). These two contributions are important to understand the data summarized in Fig. 3. The microscopic description of the remaining coefficients χ_2 and χ_3 is out of the scope of this Letter. Our analysis of the ratchet effects is based on the classical Boltzmann equation for the electron distribution function $f_{\boldsymbol{k}}$, namely,

$$\left(\frac{\partial}{\partial t} + v_{\boldsymbol{k},x}\frac{\partial}{\partial x} + \frac{\boldsymbol{F}}{\hbar}\frac{\partial}{\partial \boldsymbol{k}}\right) f_{\boldsymbol{k}}(x) + Q_{\boldsymbol{k}}^{(p)} + Q_k^{(\varepsilon)} = 0. \tag{3}$$

Here $\boldsymbol{k}$ is the in-plane electron wave vector, $\boldsymbol{F}$ is a sum of the time-dependent electric-field force $e\boldsymbol{E}(t) = 2e\mathrm{Re}[\boldsymbol{E}_0\exp(-i\omega t)]$ of the light wave and the static force $-dV(x)/dx$, ω is the light frequency, $\boldsymbol{v}_{\boldsymbol{k}} = \hbar\boldsymbol{k}/m^*$ is the electron velocity, e and m^* are the electron charge and effective mass, $Q_{\boldsymbol{k}}^{(p)}$ and $Q_k^{(\varepsilon)}$ are the collision terms responsible for the electron momentum and energy relaxation, respectively. The operator $Q_{\boldsymbol{k}}^{(p)}$ is taken in its simplest form $(f_{\boldsymbol{k}} - \langle f_{\boldsymbol{k}}\rangle)/\tau$, where τ is the momentum relaxation time and the brackets mean averaging over $\boldsymbol{k}$ directions. The operator $Q_k^{(\varepsilon)}$ acts on the distribution function averaged over the directions of $\boldsymbol{k}$ and depends only on the modulus $k = |\boldsymbol{k}|$. Equation (3) is valid for a weak and smooth potential satisfying the conditions $|V(x)| \ll \varepsilon_e$ and $q \equiv 2\pi/a \ll k_e$, where k_e is the typical electron wave vector and ε_e is the typical energy assumed to be larger than the photon energy $\hbar\omega$.

First, we start with the *polarization-independent ratchet effect*. The photocurrent contribution, insensitive to the lights' polarization, is given by the term proportional to χ_1 in Eqs. (2) and can be related to the heating of free carriers by the electromagnetic wave and constitutes the ratchet effect for unpolarized radiation. At high temperatures, where $l_e \ll a$, Eq. (3) can be reduced to the macroscopic equations for the 2DES density $N(x)$, local nonequilibrium temperature $\Theta(x)$, current density j_x and energy flux density $i_{\varepsilon,x}(x)$. Under homogeneous optical excitation these equations have the following solution $k_B\Theta = k_BT + \hbar\omega G\tau_\varepsilon$, $N(x) \equiv N(x,\Theta) = N_0 e^{-V(x)/k_B\Theta}$, where G is the Drude absorption rate per particle, τ_ε is the energy relaxation time, and N_0 is x independent. For this solution both j_x and $i_{\varepsilon,x}$ are absent, but the current j_x becomes nonzero if the generation rate G varies spatially. In patterned samples where the distance between the surface pattern and the QW is smaller than the wavelength, the required inhomogeneous distribution of the radiation electric field is expected due to near-field effects [1]. As a result, the amplitude of a plane electromagnetic field shining through the superimposed grating becomes a periodic function of x with the period a. In an asymmetrical SL, the potential $V(x)$ and the light intensity $I(x)$ are shifted relative to each other in phase; thus, the product $I(x)(dV/dx)$ averaged over space does not vanish and even unpolarized radiation yields a net current.

Let the spatial variation of G be described by $G(x) = G_0 + G_1 \cos(qx + \varphi_G)$. The steady-state generation produces a stationary periodic electron temperature $\Theta(x) - \bar{\Theta} \equiv \delta\Theta(x) = k_B^{-1}\tau_\varepsilon \hbar\omega[G(x) - G_0]$ which is accompanied by a light-induced periodic correction of the space-oscillating contribution to the electron density $\delta N(x) \approx -N_0\delta\Theta(x)/\bar{\Theta}$. In the macroscopic description the current is given by a sum of the drift and diffusion terms,

$$j_x = \mu\left\{N(x)\frac{dV(x)}{dx} + \frac{d}{dx}[k_B\Theta(x)N(x)]\right\}.$$

Although each of the terms is dependent on x, the total current j_x is x independent. The diffusion term averaged over the period d vanishes. Since the average of the product $N(x, \bar{\Theta})dV(x)/dx$ is also zero the current can be calculated as an average $\mu\overline{[dV(x)/dx]}\delta N(x)$.

For the lateral potential taken in the form $V(x) = V_1 \cos(qx + \varphi_V)$, the symmetry of the system is broken due to a phase shift between $V(x)$ and $\Theta(x)$ yielding

$$j_x = \chi_1 I = \mu N_0 \hbar q \zeta' G_0 \frac{V_1}{2k_B T}\omega\tau_\varepsilon, \tag{4}$$

where $\zeta' = (G_1/G_0)\sin(\varphi_V - \varphi_G)$ is an asymmetry parameter related to the inhomogeneous photoexcitation. The model used to derive Eq. (4) is similar to the one considered in Ref. [15] for a ratchet with sinusoidal potential and temperature variation, shifted in phase. We note that such nonequilibrium asymmetric systems with a periodic potential $V(x)$ and a periodic temperature profile $\Theta(x)$ are called the Seebeck ratchets [5]. Equation (4) shows that the current is polarization independent and increases with decreasing T, as observed in experiment.

Now we turn to the helicity dependent part and discuss the term described by γ in Eqs. (2) or A in Eq. (1). As this photocurrent contribution is driven by circularly polarized light we call it the *circular ratchet effect*. We show that such currents is generated in a lateral SL with the out-of-phase periodic potential $V(x)$ and generation $G(x)$. At $\theta_0 = 0$ the current can only be generated in the y direction. For circularly polarized radiation the χ_3 term in Eqs. (2) vanishes and the current is given by $j_y = \pm I\gamma$, with $\pm$ corresponding to the right- and left-handed radiation, respectively. The current reads

$$j_y = \frac{2e^2\tau}{m^*}\mathrm{Re}\{\overline{E^*_{0y}(x)\delta N_\omega(x)}\}, \tag{5}$$

where $\delta N_\omega(x)$ is the electron density oscillation linear in the THz electric field E_{0x}. From the continuity equation $-i\omega e\delta N_\omega + dj_{x,\omega}/dx = 0$ and the equation for the linear-response electric current $j_{x,\omega}(x)$ modulated in space the circular photocurrent is described by

$$\gamma = \frac{\pi e^2}{\hbar c n_\omega}\zeta'\mu N_0 \frac{\hbar q}{m^*}\frac{\tau}{\omega(1+\omega^2\tau^2)}\frac{V_1}{k_B T}. \tag{6}$$

The generation of a steady-state electron flow along the y axis sensitive to the degree of circular polarization P_{circ} stems from two phase shifts with respect to the periodic variation $\delta N(x, t)$: a spatial one, given by $\varphi_V - \varphi_G$ relative to $V(x)$ and a temporal one, given by $\arctan(\omega\tau)$ with respect to $E_x(t)$. This photocurrent is by factor of $2\omega\tau_\varepsilon$ smaller than the polarization-independent current, in agreement with our data shown in Fig. 3. Similarly to the polarization-independent one this current increases with the decreasing T, in line with the experiment.

To summarize, the lateral grating etched into the sample surface induces a periodical lateral potential acting on the 2DES. This grating modulates the incident radiation in the near field and hence in the plane of the 2DES, resulting in polarization-independent, circular, and linear ratchet effects. The former effect was predicted in Ref. [15] for unpolarized light. In this work we have additionally observed helicity dependent photocurrents arising due to the phase shift between periodic potential and periodic light field. Our theory describes ratchet effects for a mean free path smaller than the superlattice period. In the opposite limit, $l_e \gg a$, a new approach is required, which should be based on the microscopic Boltzmann equation with allowance for an asymmetry of the lateral potential and, possibly, miniband formation.

We thank M. M. Voronov, V. V. Bel'kov, L. E. Golub, and S. A. Tarasenko for fruitful discussions. The support from the DFG (SFB 689) is gratefully acknowledged. E. L. I. thanks the Mercator Program of the DFG for support.

[1] S. D. Ganichev and W. Prettl, *Intense Terahertz Excitation of Semiconductors* (Oxford University Press, Oxford, 2006).
[2] E. L. Ivchenko, *Optical Spectroscopy of Semiconductor Nanostructures* (Alpha Science Int., Harrow, UK, 2005).
[3] E. M. Baskin, L. I. Magarill, and M. V. Entin, Sov. Phys. Solid State **20**, 1403 (1978).
[4] V. I. Belinicher and B. I. Sturman, Phys. Usp. **23**, 199 (1980).
[5] P. Reimann, Phys. Rep. **361**, 57 (2002).
[6] P. Hänggi, F. Marchesoni, and F. Nori, Ann. Phys. (Leipzig) **14**, 51 (2005).
[7] P. Reimann, M. Grifoni, and P. Hänggi, Phys. Rev. Lett. **79**, 10 (1997).
[8] A. Lorke *et al.*, Physica (Amsterdam) **249–251B**, 312 (1998).
[9] H. Linke *et al.*, Science **286**, 2314 (1999).
[10] A. M. Song *et al.*, Appl. Phys. Lett. **79**, 1357 (2001).
[11] J. B. Majer *et al.*, Phys. Rev. Lett. **90**, 056802 (2003).
[12] L. I. Magarill, Physica (Amsterdam) **9E**, 652 (2001).
[13] A. D. Chepelianskii *et al.*, Eur. Phys. J. B **56**, 323 (2007).
[14] W. Weber *et al.*, Phys. Rev. B **77**, 245304 (2008).
[15] M. Büttiker, Z. Phys. B **35**, 177 (1979); Y. M. Blanter and M. Büttiker, Phys. Rev. Lett. **81**, 4040 (1998).
[16] S. Adachi and K. Oe, J. Electrochem. Soc. **130**, 2427 (1983).
[17] S. D. Ganichev *et al.*, Phys. Rev. Lett. **86**, 4358 (2001).